

New Multiscale Heat Transfer Techniques

SILVIA NEDEA¹, NICOLAE GOGA^{2*}, BART MARKVOORT¹, ANTON VAN STEENHOVEN¹

¹Technical University Eindhoven. Mechanical Engineering, 5600 MB Eindhoven, the Netherlands

²University of Groningen, Faculty of Natural Science, Nijenborgh 4, 9747 AG Groningen, the Netherlands

In this paper we present a new multiscale method for coupling molecular dynamics simulations (MD) with Monte Carlo (MC) simulations. The method is relevant for heat transfer phenomena at the molecular level with applicability in many domains such as polymer processing, crystallization process in moving polymer melt, complex flows near the interfaces, e.g. wetting, colloids near surfaces, drop formation, etc. First the theoretical background is described and after that simulation results between multiscale MD-MC and pure MD simulation are presented. At the end, comparisons between accuracy and computational costs of MD, MC and multiscale MD-MC simulations are outlined.

Keywords: heat transfer techniques, polymers, Monte Carlo simulations, molecular dynamics, multiscale modeling

Now-a-days there are different techniques through which heat transfer phenomena can be modeled and studied through the employment of the computational power of the clusters of computers. Among them we can mention Monte Carlo (MC) and molecular dynamics (MD) simulations. The applicability of these methods covers a large range of domains such as polymer processing [1], crystallization process in moving polymer melt [2], complex flows near the interfaces, e.g. wetting, colloids near surfaces, drop formation, to mention just a few.

Multi-scale simulations become more and more important in order to understand complex physical systems. The challenge lies in resolving physical phenomena occurring over a broad range of spatial and temporal scales [3, 4]. As conventional single method formulations can not give a good description of these phenomena, efficient multi-scale formulations are used in order to respond to this challenge. By limiting the use of an expensive atomistic model to the regions where it is needed, while using a simpler, less expensive method in the rest of the computational domain, simulations over larger time and length scale become possible.

A lot of multiscale methods have been proposed for solids [4, 5, 6], liquids [22, 15, 25, 21] and gases [8, 9, 10, 13, 19, 11, 12, 17] and a wide range of systems with important applications are governed by the fine interplay between the atomistic processes occurring within a small region of the system and the slow dynamics occurring in the bulk. These multiscale methods involve coupling of standard approaches as continuum (Navier-Stokes equation, Euler equation, etc.) and atomistic (particle) simulation methods as Direct Simulation Monte Carlo (DSMC) and Molecular Dynamics. In MD, the time evolution of a set of interacting particles is followed exactly, molecules move and collide according to the forces they exert on each other. In Monte Carlo (MC), collisions of molecules are generated stochastically with scattering rates and post-collisions determined from the kinetic theory.

Depending on the validity and applicability of these approaches on the application, several multiscale methods were proposed in the literature coupling continuum with DSMC, continuum with MD, and coupling particle simulation methods like MD-MC [16, 18, 17, 13, 22, 15, 21, 20].

In this paper we give an overview of the MC and MD methods, and then we focus on multiscale particle

simulation methods MC-MD [29, 26, 27, 28, 29, 30, 31]. We describe in detail our coupling technique and the application of the method [28], and we compare with pure MD simulations for the validity of the results [30, 29, 26, 27, 31]. Even if this paper should be regarded as an overview of this hybrid method, we give here also some new results regarding the model capabilities to handle flows at different temperature and densities. In the end we discuss about the efficiency of the method and still open points in this approach.

Experimental part

Nomenclature

In what follows, the following notations are used:

$F(x, \xi, t)$ stands for one-particle distribution;

J_E - collision integral;

n - number density;

$V_L(r)$ - Lennard-Jones;

Y - pair correlation function;

η - reduced density;

ξ - molecular velocity (m/s);

λ - mean-free path (nm);

ε - interaction strength (kJ/mol);

σ - particle size (nm);

LJ - Lennard-Jones potential;

$tsLJ$ - truncated shifted LJ potential;

c - cut-off radius;

MD - Molecular Dynamics;

MC - Monte Carlo

Monte Carlo Methods

The first simulation method used is an extended version of the Direct Simulation Monte Carlo method. The method is based on the Enskog kinetic equation [43].

This Enskog equation is an extension of the Boltzmann equation to dense fluids and has the form

$$\frac{\partial F}{\partial t} + \varepsilon \circ \nabla F = J_E(F, F), \quad (1)$$
 where $F(x, \xi, t)$ is the one-particle distribution function of the molecular velocity ξ .

The collision integral $J_E(F, F)$ keeps the same binary structure of the corresponding Boltzmann term, but the colliding molecules occupy different positions in space and the collision frequency is modified by the factor Y which

* email: n.goga@rug.nl

plays the role of an approximate pair correlation function [35, 36]. The Y function has the form:

$$Y(n) = \frac{1}{2} \frac{2 - \eta}{(1 - \eta)^2}, \quad (2)$$

where η is the reduced density.

The important macroscopic quantities that are computed in our MC simulations are the number density, the mean velocity, the temperature, the heat flux and the stress. In terms of the one-particle distribution function F , these properties can be written as follows:

$$n(x) = \int F(x, \xi) d\xi, \quad (3)$$

mean velocity

$$u(x) = 1/n(x) \int \xi F(x, \xi) d\xi, \quad (4)$$

and temperature

$$T(x) = \frac{m}{3n(x)k} \int (\xi - u)^2 F(x, \xi) d\xi, \quad (5)$$

where k is the Boltzmann constant.

Molecular Dynamics

The second simulation method is Molecular Dynamics (MD). In a MD simulation the exact particle trajectories are calculated by computing all the forces that the particles exert upon each other. These forces are described by means of interaction potentials.

A commonly used potential to describe the interactions between particles is the Lennard-Jones (LJ) potential

$$V_{LJ}(r) = \varepsilon \left[\left(\frac{2R_{vdW}}{r} \right)^{12} - 2 \left(\frac{2R_{vdW}}{r} \right)^6 \right], \quad (6)$$

where:

ε is the interaction strength

R_{vdW} , the van der Waals radius, a measure for the particle size.

The LJ potential is mildly attractive as two molecules approach each other from a distance, but strongly repulsive when they come too close. In order to simulate hard-sphere like interactions using MD, truncated shifted Lennard Jones (tsLJ) potentials were used for the interactions between gas molecules. This potential is defined as $V_{tsLJ}(r) = V_{LJ}(r) - V_{LJ}(r_c)$ if $r \leq r_c$ and 0 if $r > r_c$, where r_c is the cut-off radius.

With a cut-off radius $r_c = 2R_{vdW}$, this basically means that only the repelling part of the LJ potential is taken into account such that all the attractive interactions between particles situated at larger distances are ignored. The choice of ε determines how hard the particles are. This is shown in [29], where the hard sphere potential is compared with our potentials. For the tsLJ potential with $\varepsilon=1$ the particles are still relatively soft, i.e. the particles can partially overlap during a collision. When two particles come closer together than $2R_{vdW}$, they start to repel each other. When they come closer together, kinetic energy is converted to potential energy until all kinetic energy in the direction of the separation between the two particles has been converted.

Then the two particles move away from each other where the potential energy is converted back to kinetic energy. A second measure for the particle size is thus given by the minimal distance between the two particles during such a collision, which we will refer to as the collision diameter. This collision diameter will be different for every collision as the velocities of all particles are different, however on average this collision diameter will approximately equal that distance for which the pair interaction potential $V(r)$ equals one. As this minimum distance during a collision compares well to the size of the particles in the MC simulations we will use this collision

diameter to fix the value for R_{vdW} in equation (6). Thus, for $\varepsilon=1$ the choice $2R_{vdW} = 2^{1/6}a$ results in particles with average collision diameter a . For a stronger tsLJ potential with $\varepsilon=1000$ an average collision diameter a is obtained with the choice $2R_{vdW} = 1.005a$. These particles are very close to hard spheres and thus hardly overlap, such that the van der Waals radius is only slightly larger than $a/2$.

Periodic boundary conditions are used again in the directions parallel to the plates. The plates can be modeled again using the same thermal wall boundary conditions as used for the MC simulations. However, with MD it is also possible to simulate the walls explicitly.

Namely, an advantage of the MD method is that it is not only suited for simulating gases and liquids but also for crystals. With the MD method it is thus possible to model the walls and thus also the interaction of the gas particles with these walls explicitly.

When the walls are simulated explicitly, LJ potentials are used to simulate the interaction of the particles in these walls. For the interactions of the molecules in the solid, the standard LJ potential is used with $\varepsilon=6$ in order to keep the crystal structure of the solid intact and to prevent the wall particles to evaporate and to mix with the gas molecules.

The interactions between the wall particles and the gas particles and between gas particles mutually are modeled by weaker Lennard Jones potentials or by a truncated shifted Lennard Jones potential. Thus, in MD both explicit wall and boundary conditions can be used to model the plates. The advantage of the use of boundary conditions is that much less particles are needed in the simulation and that the MC and MD method can be compared more fair on the same basis. The advantage of the use of explicit walls is that the interaction with the wall, that can be crucial for the total behaviour, can be simulated much more accurately. Being able to include a more accurate description of the interface is a very important feature of the multiscale method.

Also from the MD simulations macroscopic properties can be derived, such as the density, the mean velocity, the temperature, the heat flux and the stress [28].

Multiscale Molecular Dynamics-Monte Carlo Methods

In order to perform more efficient simulations, we have proposed a simulation method that combines the advantages of the Molecular Dynamics and Monte Carlo simulations, where we use either MD or MC as described before [28].

How this is done is shown schematically in figure 1 for the case where MD is used in the left half of the simulation domain (regions I and II) and MC in the right half (regions III and IV).

Our simulation algorithm consists of the following steps:

- first an initial configuration for the whole system is created. The positions of the particles are randomly generated in the simulation domain, and the velocities of the particles are generated from a Maxwell-Boltzmann distribution;

- the particles in the region in which MD is performed are sent to the MD simulator and analogously the particles in the MC range are sent to the MC simulator;

- however, the MD simulation needs information from the neighboring MC particles and vice versa. This is obtained by creating an interface coupling the two subdomains. The MD simulation is extended with a buffer layer (BL_{MD}) to which the information of the MC particles in region III are copied and analogously the MC simulation is extended with a buffer layer (BL_{MC}) to which the information of the MD particles in region II are copied;

- now both the MD and the MC simulator can run in parallel. This implies that the MC simulator performs one iteration, updating the positions and velocities of all its particles. Parallel to this, the MD simulator should simulate the same time interval. Because the time step size that can be made in one MD iteration is usually small compared to the time step size in MC, we have to do a number of MD time steps for every single MC simulation step;

- the information for the whole system is now obtained by recombining regions I and II from MD with regions III and IV from MC. And the simulation can be continued with a new iteration of the multiscale procedure by restarting from step 3.

In the following we will elaborate more on the most important aspects of the method. The first important point is about updating the buffer layers after each iteration of the multiscale method. A straightforward approach is to provide the buffer layers BL_{MD} and BL_{MC} with a new copy of regions III and II respectively.

In [27], we have previously investigated the coupling between the two methods in this way which was realized by importing and exporting particles from one simulator to the other. However, as we couple two simulation methods based on a different mechanism of computing the interactions between particles, problems are encountered as expected when trying to couple the less detailed method with the more accurate method. This is the case for coupling the MC and MD particle domains.

Whereas for MD to MC particle coupling, particles from the MD domain can be imported directly into the MC domain using the exact positions and velocities, this cannot be done for MC to MD particle coupling as in MC simulations particles can overlap each other. Imported into the MD domain, this would result in very large forces, leading to a high temperature jump in the interface layer caused by energy conservation problems.

An alternative method is used for the MC to MD coupling, where macroscopic properties are copied instead of single particles. In this method the positions and velocities of the particles in the MD buffer layer BL_{MD} are kept and subsequently scaled to match the macroscopic quantities from MC region III.

To allow also gradients in these quantities, the MD buffer layer (BL_{MD}) and MC layer III are divided into subcells, and the average properties of the particles in the subcells are imported from the MC domain. To set the temperature in the buffer layer, the particle velocities in the buffer layer are rescaled per subcell according to the corresponding imported MC average temperature per subcell from region III.

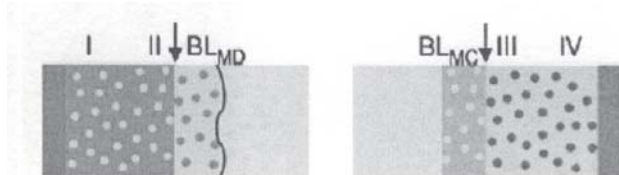


Fig. 1 The coupling of the MD and MC simulations is obtained via an interface layer. The curved-line boundary of the MD boundary layer BL_{MD} corresponds to the soft (movable) border

More details about the implementation of the buffer layers can be found in [28].

Results and discussions

Comparison Multiscale MD, MC methods for the thermal problem

We validate our multiscale MD-MC simulation results by comparing them with the pure MC and pure MD simulation

results. We have splitted the domain equally into two subdomains, one half being the MD subdomain, and the other half the MC subdomain like in figure 1. The temperature of the warm wall T_2 is twice the temperature of the cold wall T_1 .

Figure 2 shows the multiscale MD-MC simulation results for the density and temperature profile when $L=50\lambda$ and $T_2/T_1=2$, for a dense gas ($\eta=0.2$). Our simulation profiles are equal to pure MD and pure MC simulation results, proving that we can use the multiscale method to couple MD and MC simulations. In all these simulations thermal wall boundary conditions are considered both in MC and in MD, and MD particles are considered to be as previously described, having $\epsilon=1$.

Results about the deviations of multiscale method compared to pure MD results were given in [30]. Zooming in the region next to the wall, we notice that deviations of the pure MC compared to pure the MD results are increasing with η , but the multiscale simulations next to the wall still show very accurate results compared to the pure MD results. In figure 3 we see that the multiscale density profile follows very well the MD density profile, and the accuracy increases when increasing the width of the MD domain next to the wall [30]. Quantifying the deviations for $\eta=0.2$, for the example in figure 2, we find the MC deviations equal to 1.9%, while the multiscale deviations when comparing to MD results equal 0.2% [30].

In [28] we showed that the timings results of the multiscale method depend on how large is the MD domain when compared to the MC domain. The speedup when using multiscale MD-MC method for 50%MD and 50% MC is very small when compared to pure MD simulations times, but this speedup increases drastically when the bulk is larger than the region near the wall.

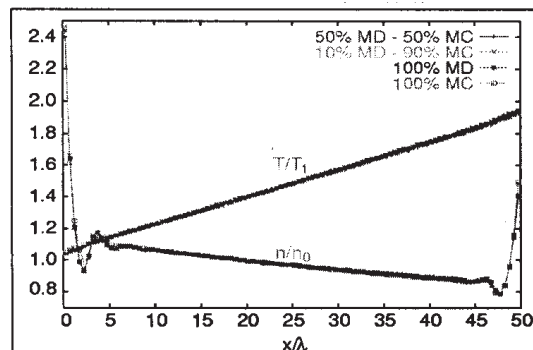


Fig. 2. The density and temperature profiles in the channel as obtained from the multiscale MD-MC simulations for $\eta=0.2$, $T_2/T_1=2$, and $L=50\lambda$. The domain is splitted in two subdomains, the left one being MD (50%), and the right one MC (50%). MD particles having $\epsilon=1$, and thermal wall boundary conditions are considered

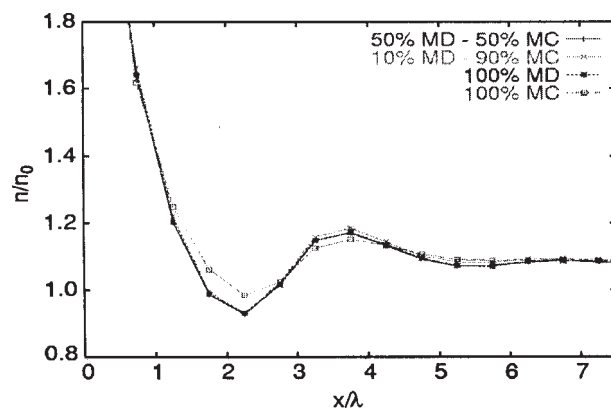


Fig. 3. Zoom-in density next to the cold wall of example in figure 2

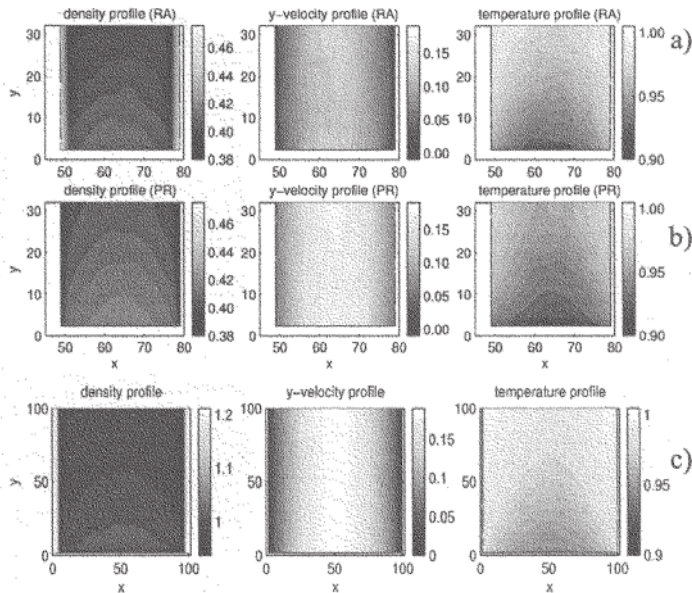


Fig 4 Density, flow velocity and temperature distributions in the channels for different sets of interaction parameters, for a cold flow imposed between the two vertical warm walls of the channels: a) MD-RA (repulsive and attractive) interaction between gas and wall particles, b) MD-PR (purely repulsive) interaction between gas and wall particles, c) MC-thermal wall boundary conditions

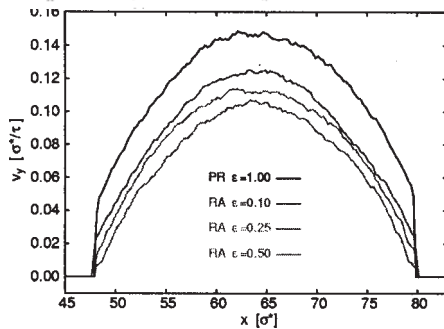


Fig 5. Flow velocity for purely repulsive (PR) and repulsive-attractive (RA) gas-wall interaction. Higher velocity profile in case of PR interactions than in case of RA interactions

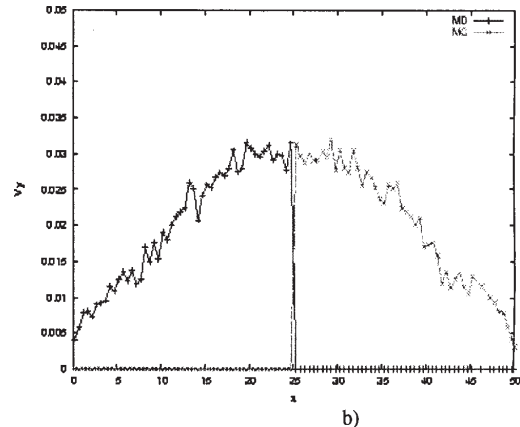
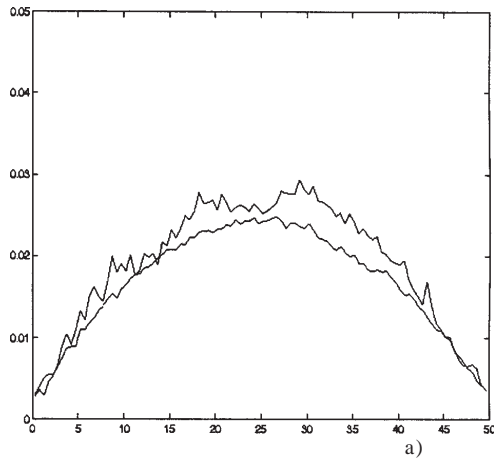


Fig 6 . Poiseuille flow in the micro/nano-channel. a) MC and MD velocity flow profiles (low line-MC, high line MD) b) multiscale simulation of the velocity flow profile

For example, when the MC domain is extended to 90% of the simulation domain and MD domain reduced to 10% of the simulation domain, the speedup of the simulations increases roughly with a factor five. We notice also that this efficiency is independent on density.

Application Micro/Nano Channel Cooling

This method is extended in order to be able to analyse heat transfer in micro/nano-channels in different flow regimes, and to more accurately simulate the solid-gas interface. A Poiseuille flow is imposed by applying an extra force on particles situated in the first 3λ of the channel. Different MC and MD models can be considered for more accurate gas-surface interactions.

In the MD model, the interactions between molecules can be pure repulsive (PR) or attractive repulsive (RA) [29],

while in MC different boundary conditions (fig. 1b) can be imposed (thermal wall, reflective, periodic, etc.).

In all the previous plots, the walls have been simulated using boundary conditions. When the walls are explicitly introduced in the simulations, the discrepancies appear even between different MD simulations where walls are either attractive (hydrophilic-RA interactions) or repulsive (hydrophobic-PR interactions).

In figure 4, a cold flow is imposed between two warm walls of a channel. Different model interactions influence the properties in the channel. The physically more realistic RA model predicts more heat transfer than the more simplified PR model. The flow velocity is higher for hydrophobic interactions than for hydrophilic ones (fig. 5).

The attraction causes hardly any slip while the repulsive causes a large slip near the wall and this results in a higher temperature of the gas in case of the attractive than in

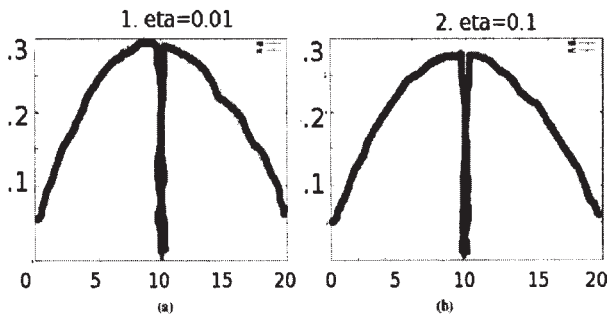


Fig 7. Profile for the flow velocity for 1) $\eta=0.01$ and 2) $\eta=0.1$

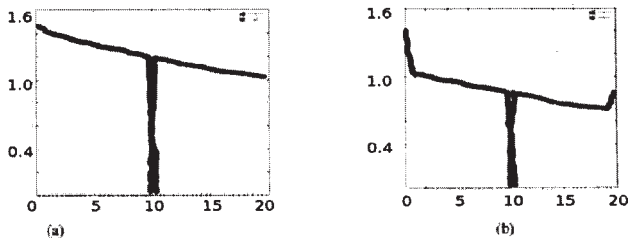


Fig 8. Multiscale results for the densities profile in a system with a) $\eta=0.01$ and b) $\eta=0.1$

case of the repulsive. Thus, although the velocity flow is smaller, looking at the temperature profiles we see that the amount of heat that can be removed is larger in case of attractive walls because of the better heat transfer over the interface. This shows once again, that the accuracy of the simulation results depends on how accurate we model the interactions between gas and wall molecules and that pure MC is not good enough to describe these effects.

In figure 6a, we compared the MC and MD velocity profiles for a Poiseuille flow. In both cases, thermal wall boundary conditions were used. Because particles are relatively soft in the MD, the MD velocity profile is slightly higher than the MC one. When increasing ϵ , going to a hard-sphere interaction, these profiles will overlap. In figure 6b we can see the multiscale simulation preliminary result of the flow in a micro-channel for a relatively higher ϵ . These profiles have the same slip near the boundaries and also the same maximum velocity. In the future, coupling more complex MD models with MC near the wall boundaries of the wall is going to be investigated.

Application of the Multiscale to study mixed flow and thermal problems for dense and dilute systems

We used the microscale approach to study behaviour in channels having the same flow velocity and a temperature gradient between the warm and the cold wall ($T_1/T_2=1/2$). Two different systems were considered, a dense ($\eta=0.1$) and a dilute one ($\eta=0.01$). The idea was to check the heat fluxes in the two systems. To generate the same velocity, we applied an adjusted correspondingly force on the y direction such that the velocity profiles for both systems in figure 7 look similar.

The densities obtained using the Multiscale simulation in figure 8 validate our simulations results as they are similar to our previous results obtained for these systems using full MD simulations [28].

The heat fluxes in the channel for the dense gas compare very good with the results obtained from pure MD simulations in [28]. The ratio between the heat flux from the dense and the dilute gas was computed and it is around 0.25/0.17 (fig. 9) even if the ratio of the densities is equal to 10.

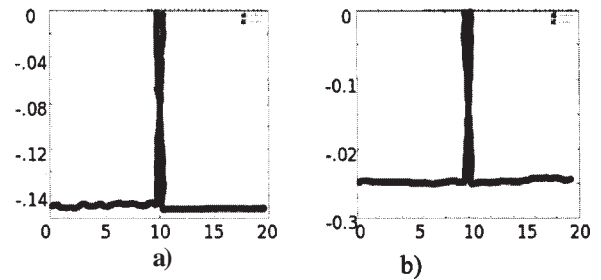


Fig 9 . Multiscale results for the heat flux profiles in a system with a) $\eta=0.01$ and b) $\eta=0.1$

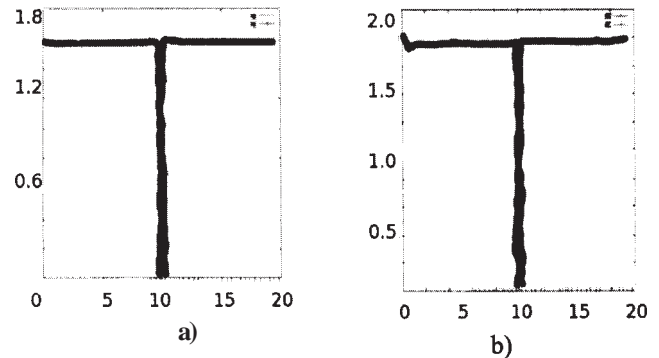


Fig 10 . Multiscale results for the heat flux profiles in a system with a) $\eta=0.01$ and b) $\eta=0.1$

The pressure results are also a bit intriguing (fig. 10). For a dense gas the pressure is lower than the pressure computed from pure MD simulations in [2]. These discrepancies can be explained by the fact that in [28], the MD molecules were hard spheres with $\epsilon=1000$ and in our simulations epsilon is much smaller ($\epsilon=100$) having thus an impact on the pressure in the system. More simulations are going to be done with $\epsilon=1000$ in order to check the behaviour of the pressure and heat flux for dilute and dense systems.

Conclusions

MD-continuum methods are presented and major issues are discussed. A new multiscale method based on coupling particle simulation methods was introduced. This method couples MD near boundaries for the accuracy of the interaction with the wall, and MC in the bulk because of the low computational costs. This is a promising technique to investigate heat transfer at atomistic level with applications in different domains starting from polymer processing till investigating the phenomena in the gas-surface interface .

References

1. DAWSON, A., RIDES, M., CRISPIN, A., *Polymeric Materials IAG*, 2008
2. EDER, G., JANESCHITZ-KRIEGL, H., LIEDAUER, *Progress in Polymer Science*, **15**, 1990, p. 629
3. GOGA, N., COSTACHE, S., MARRINK, S. *Materiale Plastice*, **46**, 2009, p. 53
4. GOGA, N., COSTACHE, S., MARRINK, S. *Materiale Plastice*, **46**, 3, 2009, p. 220
5. ABRAHAM, FF., BROUGHTON, JQ., BERNSTEIN, N., KAXIRAS, E., *Europhys.Lett.*, **44**, 1998, p. 783
6. RUDD, R.E., BROUGHTON, J.Q., *Phys. Status Solidi B*, **217**, 2000, p. 251
7. SHENOY, V.B., MILLER, R., TAMOR, E., RODNEY, D., ORTIZ, M., *J.Mech. Phys. Solid*, **47**, 1999, p. 611
8. ALDER, B.J., *Phys. A*, **240**, 1997, p. 193
9. AKTAS, O., ALURU, N.R., *J.Comput.Physics*, **178**, 2002, p. 342
10. BOURGAT, J., TALLEC, P.L.E., TIDRIRI, M., *J.Comput. Phys.*, **127**, 1996, p.227

11. TALLEC, P.L.E., MALLINGER, F., *J.Comput.Phys.*, **136**, 1997, p.51
12. ROVEDA, R., GOLDSTEIN, D.B., VARGHESE, P.L., *J.Spacecrafts and Rockets*, **37**, 2000, p. 753
13. GARCIA, A.L., BELL, J.B., CRUTCHFIELD, W.Y., ALDER, B.J., *J.Comput. Phys.*, **154**, 1999, p. 134
14. DELGADO-BUSCALIONI, R., COVENEY, P.V., *Journal of Chemical Physics*, **119**, 2003, p. 978
15. HADJICONSTANTINO, N.G., *Journal of Computational Physics*, **154**, 1999, p. 245
16. EGGERS, J., BEYLICH, A., *Progress in Astronautics and Aeronautics*, **159**, 1994, p. 166
17. WADSWORTH, D.C., ERWIN, D.A. *AIAA Paper 90-1690*, 1990
18. HASH, D.B., HASSAN, H., *AIAA Paper 95-0410*, 1995
19. HASH, D.B., HASSAN, H., *AIAA Paper 96-0353*, 1996
20. O'CONNELL, S.T., PA. THOMPSON, *Phys.Rev.E* **52**, 1995
21. HADJICONSTANTINO, N., PATERA, A.T., *Int.J.Modern Physics C*, **8**, 1997, p. 967
22. FLEKKOY, E.G., WAGNER, G., FEDER, J., *Europhys. Lett.*, **52**, 2000, p. 271
23. GARCIA, A.L., BELL, J.B., CRUTCHFIELD, W.Y., ALDER, B.J., *J. Comput.Phys.*, **154**, 1999, p. 134
24. DELGADO-BUSCALIONI, R., COVENEY, P.V., *Phys. Rev. E*, **67**, 2003, p. 046704
25. LI, J., LIAO, D., YIP, S. *Phys.Rev. E*, **57**, 1998, p. 7259
26. NEDEA, S.V., MARKVOORT, A.J., FRIJNS, A.J.H., VAN STEENHOVEN, A.A., HILBERS, P.A.J., *Int.J.Thermal Sci*, 2006
27. FRIJNS, A.J.H., NEDEA, S.V., MARKVOORT, A.J., VAN STEENHOVEN, A.A., HILBERS, P.A.J., *Int.J.Multiscale Comp.Eng*, 2006
28. NEDEA, S.V., MARKVOORT, A.J., FRIJNS, A.J.H., VAN STEENHOVEN, A.A., HILBERS, P.A.J. *Phys. Rev.E*, **72**, 2005, p. 016705
29. MARKVOORT, A.J., HILBERS, P.A.J., NEDEA, S.V., *Phys.Rev.E*, **71**, 2005, p. 066702
30. NEDEA, S.V., FRIJNS, A.J.H., MARKVOORT, A.J., VAN STEENHOVEN, A.A., HILBERS, P.A.J., *ICMM03, ASME, Toronto, Canada, CD*, 2005
31. NEDEA, S.V., FRIJNS, A.J.H., VAN STEENHOVEN, A.A., JANSEN, A.P.J., *ICMM02, ASME, Rochester US*, 2004, p. 289
32. LIONS, P.L., *First International Symposium on Domain Decomposition Methods for Partial Differential Equations*, edited by R.Glowinski, G.Golub, G.Meurant, J.Periaux, SIAM, Philadelphia, 1988, p.1.
33. FRENKEL, D., SMITH, B. *Understanding Molecular Sim.*, Academic Press, London, 1996
34. BIRD, G.A., *Molecular Gas Dynamics and Direct Simulations of Gas flows*. Clarendon Press, Oxford, 1994.
35. FREZZOTTI, A., *J.Mech.B/Fluids*, **18**, 1999, p. 103
36. FREZZOTTI, A., *Phys.Fluids*, **9**, 1997, p. 1329
37. KUCABA-PIETA, A., ZBIGNIEW WALENTA, Z., *Int.J.Turbulence*, **10**, 2004, p. 77
38. RESIBOIS, P., DELENEER, M., *Classical Kinetic Theory of Fluids*. Wiley, NY, 1977
39. CARNAHAN, N.F., STARLING, K.E., *J.Chem.Phys.*, **51**, 1969, p: 635
40. CERCIGNANI, C., *Mathematical methods in kinetic theory*. Plenum, NY, 1990.
41. BERENDSEN, H.J.C., POSTMA, J.P.M., VAN GUNSTEREN, W.F., DINOLA, A., HAAK, J.R., *J.Chem. Phys.*, **81**, 1984, p. 3684
42. ESSELINK, K., HILBERS, P.A.J., *J.C. Phys.*, **106**, 1992, p. 108
43. ENSKOG., D., *Kinetische Theorie der Waerme Leitung*, *Kungl.Svenska Vetenskapsakad. Handl.*, 63:3-44, 1922

Manuscript received: 17.03.2011